You might find this additional info useful...

This article cites 73 articles, 35 of which can be accessed free at:
http://ajpheart.physiology.org/content/298/2/H385.full.html#ref-list-1

This article has been cited by 3 other HighWire hosted articles

Cation dyshomeostasis and cardiomyocyte necrosis: the Fleckenstein hypothesis revisited
Brian J. Borkowski, Yaser Cheema, Atta U. Shahbaz, Syamal K. Bhattacharya and Karl T. Weber
Eur Heart J, March 12, 2011; .
[Abstract] [Full Text] [PDF]

Calcium and zinc dyshomeostasis during isoproterenol-induced acute stressor state
Atta U. Shahbaz, Tieqiang Zhao, Wenyuan Zhao, Patti L. Johnson, Robert A. Ahokas, Syamal K. Bhattacharya, Yao Sun, Ivan C. Gerling and Karl T. Weber
Am J Physiol Heart Circ Physiol, February , 2011; 300 (2): H636-H644.
[Abstract] [Full Text] [PDF]

Updated information and services including high resolution figures, can be found at:
http://ajpheart.physiology.org/content/298/2/H385.full.html

Additional material and information about *AJP - Heart and Circulatory Physiology* can be found at:
http://www.the-aps.org/publications/ajpheart

This infomation is current as of July 20, 2011.

Temporal responses to intrinsically coupled calcium and zinc dyshomeostasis in cardiac myocytes and mitochondria during aldosteronism

German Kamalov,[1] Robert A. Ahokas,[2] Wenyuan Zhao,[1] Atta U. Shahbaz,[1] Syamal K. Bhattacharya,[1] Yao Sun,[1] Ivan C. Gerling,[3] and Karl T. Weber[1]

[1]*Division of Cardiovascular Diseases,* [2]*Department of Obstetrics and Gynecology, and* [3]*Division of Endocrinology, University of Tennessee Health Science Center, Memphis, Tennessee*

Kamalov G, Ahokas RA, Zhao W, Shahbaz AU, Bhattacharya SK, Sun Y, Gerling IC, Weber KT. Temporal responses to intrinsically coupled calcium and zinc dyshomeostasis in cardiac myocytes and mitochondria during aldosteronism. *Am J Physiol Heart Circ Physiol* 298: H385–H394, 2010. First published November 13, 2009; doi:10.1152/ajpheart.00593.2009.—Intracellular Ca^{2+} overloading, coupled to induction of oxidative stress, is present at 4-wk aldosterone/salt treatment (ALDOST). This prooxidant reaction in cardiac myocytes and mitochondria accounts for necrotic cell death and subsequent myocardial scarring. It is intrinsically linked to increased intracellular zinc concentration ($[Zn^{2+}]_i$) serving as an antioxidant. Herein, we addressed the temporal responses in coupled Ca^{2+} and Zn^{2+} dyshomeostasis, reflecting the prooxidant-antioxidant equilibrium, by examining preclinical (*week 1*) and pathological (*week 4*) stages of ALDOST to determine whether endogenous antioxidant defenses would be ultimately overwhelmed to account for this delay in cardiac remodeling. We compared responses in cardiomyocyte free $[Ca^{2+}]_i$ and $[Zn^{2+}]_i$ and mitochondrial total $[Ca^{2+}]_m$ and $[Zn^{2+}]_m$, together with biomarkers of oxidative stress and antioxidant defenses, during 1- and 4-wk ALDOST. At *week 1* and compared with controls, we found: *1*) elevations in $[Ca^{2+}]_i$ and $[Ca^{2+}]_m$ were coupled with $[Zn^{2+}]_i$ and $[Zn^{2+}]_m$; *2*) increased mitochondrial H_2O_2 production, cardiomyocyte xanthine oxidase activity, and cardiac and mitochondrial 8-isoprostane levels, counterbalanced by increased activity of antioxidant proteins, enzymes, and the nonenzymatic antioxidants that can be considered as cumulative antioxidant capacity; some of these enzymes and proteins (e.g., metallothionein-1, Cu/Zn-superoxide, glutathione synthase) are regulated by metal-responsive transcription factor-1; and *3*) although these augmented antioxidant defenses were sustained at *week 4*, they fell short in combating the persistent intracellular Ca^{2+} overloading and marked rise in cardiac tissue 8-isoprostane and mitochondrial transition pore opening. Thus a coupled Ca^{2+} and Zn^{2+} dyshomeostasis occurs early during ALDOST in cardiac myocytes and mitochondria that regulate redox equilibrium until *week 4* when ongoing intracellular Ca^{2+} overloading and prooxidants overwhelm antioxidant defenses.

aldosterone; oxidative stress; antioxidants

MORE THAN FOUR DECADES ago, Fleckenstein (25) originally proposed that intracellular Ca^{2+} overloading of cardiomyocytes and their mitochondria, coupled with a loss of high-energy-rich phosphates, account for irreversible structural damage to these organelles and subsequent cellular necrosis. They validated their hypothesis using a single dose of a catecholamine to induce an acute Ca^{2+} overload and verapamil, a Ca^{2+} antagonist later proved to be a Ca^{2+} channel blocker, to prevent ensuing cardiac pathology. Nakayama et al. (56) have revalidated Fleckenstein's hypothesis of intracellular Ca^{2+} overloading-induced cardiomyocyte necrosis as a primary mediator of heart failure. Using transgenic mice with overexpressed sarcolemmal L-type Ca^{2+} channels, they found progressive necrotic death of these cells, which led to ventricular dysfunction and shortened survival of these rodents. Isoproterenol, a synthetic catecholamine, accelerated these adverse events, whereas an L-type Ca^{2+} channel blocker or β_1-adrenergic receptor antagonist prevented them altogether. We demonstrated the pathogenic roles of excessive intracellular Ca^{2+} accumulation (EICA; Ref. 10) as well as the cardioprotective properties of diltiazem (12) and parathyroidectomy (57) in the cardiomyopathy found in the Syrian hamster with muscular dystrophy. Subsequent studies with ischemia-reperfusion (I/R) injury would identify the induction of oxidative stress that accompanies acute EICA in leading to cardiomyocyte necrosis (38). The necrotic cell death pathway that occurs in cardiomyocytes in response to catecholamines or I/R injury is now recognized to initiate in mitochondria and is mediated via the opening of the mitochondrial permeability transition pore (mPTP), which is regulated by cyclophilin D and for which inhibition is cardioprotective (18, 38, 42, 56).

Using 4-wk aldosterone/salt treatment (ALDOST) in rats to simulate chronic, inappropriate (relative to dietary Na^+), homeostatic activation of the renin-angiotensin-aldosterone system that accompanies reduced renal perfusion in patients with heart failure, we identified parathyroid hormone (PTH)-mediated subacute EICA in cardiomyocytes and mitochondria of the normal heart as associated with the induction of oxidative stress at these cellular and subcellular sites together with cardiomyocyte necrosis and myocardial scarring (19, 66, 69). Cotreatment with the following prevents this prooxidant state: spironolactone, an aldosterone receptor antagonist, attenuates the heightened urinary and fecal excretion of Ca^{2+} and consequent appearance of ionized hypocalcemia to prevent secondary hyperparathyroidism (SHPT; Ref. 19); a dietary Ca^{2+} supplement, together with vitamin D, to prevent hypocalcemia and SHPT (33); parathyroidectomy (69); a calcimimetic that resets the Ca^{2+}-sensing threshold of the parathyroid glands to prevent SHPT (60); amlodipine, an L-type Ca^{2+} channel blocker (2); or an antioxidant (66). Thus PTH-mediated intracellular Ca^{2+} overloading and the induction of oxidative stress are integral pathophysiological responses that account for adverse cardiac remodeling during chronic aldosteronism. Several additional lines of investigation demonstrate the cardiac fibrosis seen with ALDOST is not related to aldosterone per se. First, fibrosis does not appear when rats are treated with aldosterone together with dietary Na^+ deprivation (14). Sec-

ond, fibrosis is not found in transgenic mice with a cardiospecific overexpression of aldosterone synthase that accounts for increased aldosterone levels in the myocardium (28). Third, elevations in plasma prorenin and aldosterone found in Cyp1a1-Ren2 transgenic rats are not accompanied by cardiac fibrosis (58a). Collectively, these studies further underscore the importance of inappropriate (relative to dietary Na^+ intake) elevations in plasma aldosterone in predisposing the myocardium to reparative fibrosis through PTH-mediated intracellular Ca^{2+} overloading and induction of oxidative stress that regulate mPTP opening with ensuing necrotic cell death. As we (19) reviewed previously, urinary Ca^{2+} excretion occurs in the distal segment of the nephron and is dietary Na^+-dependent. Hypercalciuria accompanies the short-term treatment of humans or animals with a mineralocorticoid and dietary Na^+ (17, 29, 50, 59, 64, 75). Increased dietary Na^+ intake is calciuric with enhanced excretory Ca^{2+} losses, accentuated by prior uninephrectomy, leading to plasma-ionized hypocalcemia and SHPT.

It is noteworthy we found that subacute intracellular Ca^{2+} overloading associated with ALDOST to be accompanied by a concomitant antioxidant response invoked by the intrinsic coupling of Ca^{2+} and Zn^{2+} dyshomeostasis, which includes Zn^{2+} entry, via L-type Ca^{2+} channels to a lesser extent and primarily by the upregulated expression of Zn^{2+} transporters (26, 44). Increased cytosolic free Zn^{2+} serves to activate its sensor, the metal-responsive transcription factor (MTF)-1, to regulate the expression of endogenous antioxidant defenses including metallothionein (MT)-1, Cu/Zn-SOD, and glutathione synthase (5, 44). In this context, we also found the cotreatment of ALDOST with a $ZnSO_4$ supplement to prevent cardiomyocyte necrosis and scarring (26). Thus the pathophysiological balance between prooxidants and antioxidants appears to dictate the fate of cardiomyocytes during chronic aldosteronism, although its mechanism of action distinctly differs from the acute EICA seen with catecholamines or I/R injury, where upregulated antioxidant defenses are immediately overwhelmed.

To gain further mechanistic insights into Ca^{2+} and Zn^{2+} dyshomeostasis in cardiac myocytes and mitochondria and the relative interplay between oxidative stress and antioxidant defenses before and during the appearance of cardiac pathology, *weeks 1* and *4* of ALDOST, respectively, the framework of the present study was designed. Herein, we sought to determine the temporal responses in prooxidants [intracellular calcium concentration ($[Ca^{2+}]_i$) and mitochondrial calcium concentration ($[Ca^{2+}]_m$)] and antioxidants ($[Zn^{2+}]_i$ and $[Zn^{2+}]_m$) relative to the redox state of cardiac myocytes and mitochondria present at *week 1* ALDOST, the preclinical stage, and at *week 4*, the pathological stage, coincident with myocardial scarring, a footprint of prior cardiomyocyte necrosis that appears throughout the right and left heart independent of hemodynamic factors (65). By targeting this time course, we explored whether the rise in intracellular Ca^{2+} and Zn^{2+} occurred early and was accompanied by a persistent induction of oxidative stress and upregulation of antioxidant defenses, which was then overwhelmed by the increased rate of reactive oxygen species (ROS) and nitrogen species generation. Alternatively, there could be a putative progressive rise in these intracellular cations that culminate in an overall prooxidant-antioxidant imbalance at *week 4*. To test these hypotheses, we examined

cardiac myocytes and mitochondria harvested from hearts obtained at *weeks 1* and *4* ALDOST and monitored: $[Ca^{2+}]_i$ and $[Zn^{2+}]_i$; $[Ca^{2+}]_m$ and $[Zn^{2+}]_m$; together with biomarkers of oxidative stress and antioxidant defenses and propensity for mPTP opening. Unoperated, untreated, age-/sex-matched rats served as controls.

METHODS

Animal Model

Eight-week-old male Sprague-Dawley rats were used throughout this series of experiments approved by our institution's Animal Care and Use Committee. Unoperated, untreated age-/sex-matched rats served as controls. As reported previously and following uninephrectomy, an osmotic minipump containing aldosterone was implanted subcutaneously. It releases aldosterone (0.75 µg/h) to raise circulating aldosterone levels to those commonly found in human congestive heart failure (CHF) and suppresses plasma renin activity and circulating levels of angiotensin II. Drinking water was fortified with 1% NaCl and 0.4% KCl to prevent hypokalemia. A detailed accounting of this ALDOST model, including various controls (e.g., uninephrectomy, aldosterone, or 1% NaCl treatment alone) has been reported elsewhere (44, 72). We (13, 66) also have extensively described the cardiac pathology that first appears at *week 4* ALDOST, and, therefore, it is not repeated herein. In brief, the adverse myocardial structural remodeling involving the right and left heart that accompanies ALDOST is not a consequence of hemodynamic factors or aldosterone per se (72). Instead, cardiomyocyte necrosis with resultant reparative fibrosis is the result of intracellular Ca^{2+} overloading and oxidative stress mediated by SHPT (reviewed in Ref. 45).

Isolation of Cardiomyocytes and Mitochondria

Cardiomyocytes were harvested by retrograde collagenase perfusion of the crystalloid perfused heart, and mitochondria were isolated by differential centrifugation of whole heart homogenates. The purity of mitochondrial preparation was assessed by flow cytometry and mitochondrial-specific dye MitoTracker Red (Invitrogen, Eugene, OR) as we (26) previously reported. Given the paucity of mitochondrial population density in endothelial and smooth muscle cells and fibroblasts, we speculate that overall these cells may not be a likely source of contamination. Membrane integrity of isolated mitochondria was assessed using a commercially available kit per the manufacturer's instructions (Invitrogen). Mitochondria were stained with cationic dye JC-1 followed by flow cytometry with and without mitochondrial membrane potential disrupter CCCP.

Cardiomyocyte Cytosolic Free $[Ca^{2+}]_i$ and $[Zn^{2+}]_i$

Cytosolic free Ca^{2+} concentration ($[Ca^{2+}]_i$) was measured ratiometrically using the Ca^{2+}-specific fluorophore Fura-2 (Invitrogen) as we (2, 3) have previously reported. Cytosolic free Zn^{2+} concentration ($[Zn^{2+}]_i$) of viable cardiomyocytes was measured by 2-color flow cytometry (BD FACSCalibur; Becton Dickinson, Franklin Lakes, NJ) using zinc-specific dye FluoZin-3 (Invitrogen), and propidium iodide (Sigma, St. Louis, MO) was used for detection of the nonviable cells as we (26) reported previously.

Mitochondrial Total $[Ca^{2+}]_m$ and $[Zn^{2+}]_m$

Total calcium and zinc concentration ($[Ca^{2+}]_m$ and $[Zn^{2+}]_m$) in cardiac mitochondria were determined by flame atomic spectroscopy and expressed as nanograms per milligram mitochondrial protein as previously described (11).

mPTP Opening

mPTP opening was determined by Ca^{2+}-induced swelling of isolated cardiac mitochondria according to Baines et al. (7). As reported

by these investigators, only the 200 μM Ca^{2+} concentration provided a reproducible and stable decrease in mitochondrial optical density. This decrease in optical density was completely prevented after preincubation with 30 nM cyclosporine A (CsA), thus confirming the specificity of the mPTP opening assay.

Oxidative Stress: Prooxidants

8-Isoprostane. Mitochondrial and cardiac tissue total 8-isoprostane (free and esterified) levels were measured using a competitive enzyme immunoassay kit (Cayman Chemical, Ann Arbor, MI) according to the manufacturer's protocol and as reported by us previously (26).

Mitochondrial H_2O_2 production. Mitochondrial ROS production is potentiated by a rise in intramitochondrial $[Ca^{2+}]$, partially through stimulation of Krebs cycle enzymes with increased flux of electrons to the respiratory chain. To measure the release of H_2O_2 from isolated cardiac mitochondria stimulated by succinate, the Amplex Red (Invitrogen) protocol of Mohanty et al. (54) was used with minor modifications as previously reported by us (44).

Xanthine oxidase activity. Xanthine oxidase (XO) is another well-established source of ROS in cardiac myocytes. Xanthine dehydrogenase/oxidase catalyzes the final two steps of purine catabolism with formation of the end product, uric acid, from hypoxanthine and xanthine. The mammalian enzyme is synthesized as a dehydrogenase (XDH) that uses NAD^+ as the electron acceptor, but it can also be converted into an oxidase (XO). The oxidase form consumes molecular oxygen as the electron acceptor and releases substantial amounts of superoxide anions ($O_2^{\cdot-}$) and hydrogen peroxide (H_2O_2) under certain conditions (e.g., I/R injury). Reversible conversion into XO may also take place readily through sulfhydryl group oxidation (21). However, irreversible conversion occurs through proteolytic cleavage and is shown to be regulated by intracellular Ca^{2+} (51, 52). XO activity was determined in cardiomyocyte extracts using an Amplex Red kit (Invitrogen). Briefly, 50 μl of cell homogenate was incubated in a microplate with 50 μl of working solution containing 100 μM Amplex Red, 0.4 U/ml horseradish peroxidase, and 200 μM xanthine. Samples were incubated at 37°C for 30 min, and absorbance was measured at 570 nm. To account for background correction, absorbance was also determined before sample incubation and subtracted from the final absorbance. XO activity was calculated using the standard curve and expressed in milliunits per milligram protein.

Oxidative Stress: Antioxidants

Glutathione peroxidase activity. Glutathione peroxidase (GSHPx) activity and GSSG were measured in cardiac myocytes and isolated mitochondria as previously reported by us (44).

Cu/Zn-SOD and MnSOD activity. Total Cu/Zn- and MnSOD activities in mitochondria and cardiac myocytes were measured spectrophotometrically as previously reported by us (44).

GSSG. GSSG in cardiomyocytes and isolated mitochondria were measured as reported previously by us (44).

Total antioxidant capacity. Total antioxidant capacity (TAC) of cardiac myocytes and isolated mitochondria was measured using a commercially available reagent kit (Cayman Chemical). The TAC provides more relevant biological information compared with that obtained by the measurement of individual components, as it represents the cumulative contributions from all antioxidants present in tissue, such as proteins (e.g., albumin, ceruloplasmin) and small molecules, including ascorbic acid, α-tocopherol, β-carotene, GSSG, uric acid, and bilirubin. This assay relies on the capacity of the sample-derived antioxidants to inhibit the oxidation of 2,2'-azino-di-(3-ethylbenzthiazoline sulfonate) (ABTS) to $ABTS^+$ by metmyoglobin. The capacity of the antioxidants present in the sample to prevent ABTS oxidation is compared with that of Trolox, a water-soluble tocopherol analog, and is quantified as molar Trolox equivalents per milligram protein.

Gene Microarray Analysis

Myocardial tissue was harvested from untreated, age-/sex-matched controls after 1 and 4 wk of ALDOST. The tissue was immersed and stored in RNA preservation agent (RNAlater), and then a TRI reagent (TRIzol) was added, the tissue was homogenized, and RNA was extracted as previously described (30, 31). Gene expression analysis was carried out using Affymetrix expression arrays to evaluate the changes in mRNA expression by comparing left ventricular tissue obtained from controls with 1- and 4-wk ALDOST-treated rats. We analyzed 6 independent samples from each of the 3 groups on the MOE230.2 expression array (Affymetrix), which revealed expression levels of >31,000 probe sets. Affymetrix gene expression analysis and data normalization have been extensively described by us previously (30, 31). Nine genes (from the 31,000 probe sets) were selected for analysis based on being antioxidant enzymes present on the expression array and having significant expression levels in the samples.

Immunoblotting

For immunoblotting, cardiomyocytes were lysed with SDS-urea buffer (40 mM HEPES, 4 M urea, 1% SDS, 75 mM Tris, pH 7.4). From each sample, 20 μg of total protein was separated on 10% SDS-polyacrylamide gels and transferred to a nitrocellulose membrane according to standard procedures. The nonspecific protein binding in membrane was blocked by 5% nonfat milk in TBST (0.05% Tween 20) for 1 h. Incubation with the primary antibodies to rabbit polyclonal anti-MTF-1 (1:1,000; Santa Cruz Biotechnology, Santa Cruz, CA) and mouse monoclonal anti-GAPDH (1:10,000; Chemicon, Temecula, CA) were carried out overnight at 4°C. Immunodetection was achieved using the horseradish peroxidase-conjugated anti-mouse or anti-rabbit IgG (1:10,000; Sigma), and bands were visualized with the enhanced chemiluminescence (ECL) system. To quantitate protein expression, optical density of the protein bands was measured using ImageJ software [National Institutes of Health (NIH), Bethesda, MD]. Protein loading was normalized using GAPDH as housekeeping protein. Immunoblotting data were presented as fold change relative to control cardiomyocytes.

Statistical Analysis

Group data are presented as means $\pm$ SE. Data were analyzed by the Mann-Whitney rank sum test using SigmaStat statistical software (version 2.0; Systat Software, Point Richmond, CA). Expression levels of the nine antioxidant genes in ALDOST rats from the expression arrays were normalized to the mean of their expression in control samples and presented as fold change. We analyzed fold change data by a one-way ANOVA. Significant differences between individual group means were assigned when P values were <0.05.

RESULTS

Coupled Ca^{2+} and Zn^{2+} Dyshomeostasis

Cardiomyocytes. Compared with controls (29 $\pm$ 4 nM), cytosolic free $[Ca^{2+}]_i$ in cardiomyocytes was already increased ($P < 0.05$) by *week 1* ALDOST (70 $\pm$ 5 nM) and remained elevated ($P < 0.05$) at *week 4* (80 $\pm$ 5 nM). This early and persistent Ca^{2+} overloading of cardiomyocytes was also accompanied by a persistent increase of $[Zn^{2+}]_i$ in these cells (Fig. 1). Compared with controls (0.76 $\pm$ 0.12 nM), cytosolic $[Zn^{2+}]_i$ was significantly increased ($P < 0.05$) by *week 1* (1.77 $\pm$ 0.09 nM) and *week 4* (1.64 $\pm$ 0.08 nM) ALDOST.

Mitochondria. As seen in Fig. 2, the total Ca^{2+} concentration in mitochondria $[Ca^{2+}]_m$ harvested from control hearts was 47.9 $\pm$ 4.9 ng/mg mitochondrial protein, whereas that at *weeks 1* and *4* of ALDOST (89.5 $\pm$ 5.7 and 103.4 $\pm$ 10.4
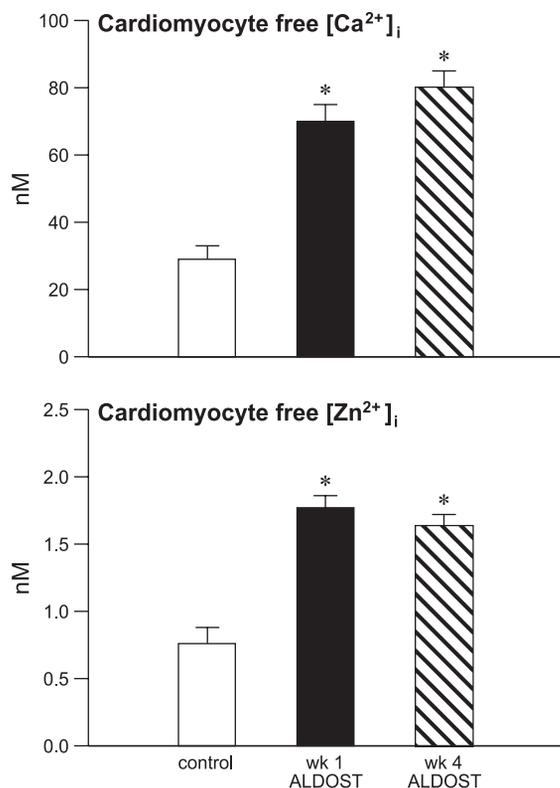
Fig. 1. Cardiomyocyte cytosolic free intracellular calcium concentration ($[Ca^{2+}]_i$) and intracellular zinc concentration ($[Zn^{2+}]_i$) harvested from control hearts as well as at *weeks 1* and *4* of aldosterone/salt treatment (ALDOST). *$P < 0.05$ vs. controls.

ng/mg mitochondrial protein, respectively) were elevated significantly ($P < 0.05$). Likewise, mitochondrial total zinc was 39.7 ± 1.0 and 41.6 ± 2.7 ng/mg mitochondrial protein at 1- and 4-wk ALDOST, respectively, and were significantly increased ($P < 0.05$) compared with controls (26.3 ± 2.8 ng/mg mitochondrial protein).

Biomarkers of Oxidative Stress

In cardiomyocytes, two major sources of ROS are mitochondria and cytosolic XO.

Mitochondrial production of H_2O_2. As seen in the *top* of Fig. 3, succinate-stimulated mitochondrial production of H_2O_2 in controls (91.0 ± 13.4 pmol·mg mitochondrial protein^{-1}·min^{-1}) was already increased ($P < 0.05$) at *week 1* ALDOST (118.3 ± 8.4) and rose further ($P < 0.05$) at *week 4* (157.6 ± 13.2), implicating that induction of oxidative stress ensued by *week 1* and was further exacerbated by *week 4*.

Mitochondrial 8-isoprostane. Mitochondrial 8-isoprostane levels (Fig. 3, *bottom*) were also increased ($P < 0.05$) during ALDOST. A marked temporal rise in mitochondrial 8-isoprostane was seen at *week 1* (878.7 ± 95.7 pmol/mg mitochondrial protein), and it remained significantly elevated at *week 4* (323.5 ± 26.8) compared with controls (124.6 ± 9.3).

XO activity. XO activity in cardiomyocytes (Fig. 4) harvested from hearts at *week 1* (2.08 ± 0.51 mU/mg protein) and *week 4* (2.93 ± 0.58) ALDOST was significantly increased ($P < 0.05$) compared with that found in controls (1.48 ± 0.14).

Similarly, the mRNA expression for xanthine dehydrogenase was also increased ($P < 0.05$) at both *week 1* and *4* ALDOST compared with controls (Table 1).

Cardiac 8-isoprostane. Oxidative damage with lipid peroxidation in the myocardium is reflected by increased 8-isoprostane tissue levels. At *week 1* ALDOST, the 8-isoprostane level (46.4 ± 9.5 pmol/mg protein) was increased ($P < 0.05$) compared with control hearts (32.8 ± 5.8), although there was no morphological evidence of myocardial scarring at this preclinical stage. Coincident with the appearance of scarring, a marker of necrosis, at *week 4* ALDOST as reported previously (66), cardiac tissue 8-isoprostane levels (341.8 ± 50.1 pmol/mg protein) were markedly increased above the control levels ($P < 0.01$) as well as at *week 1* of ALDOST ($P < 0.01$).

Antioxidant Defenses

The induction of oxidative stress seen in the heart at *weeks 1* and *4* ALDOST, contemporaneous with intracellular Ca^{2+} overloading, was accompanied by the upregulated transcription ($P < 0.05$) of multiple antioxidant enzymes. MTF-1, the intracellular Zn^{2+} sensor, is activated by increased cytosolic $[Zn^{2+}]_i$ in ALDOST (Fig. 1) compared with controls (1.0 ± 0.4). The MTF-1 protein level was increased (1.9 ± 0.2) at *week 1* and (2.7 ± 0.2) at *week 4* ALDOST. Activated MTF-1 then translocates to the nucleus, where it induces the transcription of several antioxidant genes, such as MT-1 and glutathione synthase (Table 1). These values represent the fold increase relative to controls with the assigned value of 1.00. The rise in MT-1 protein seen at *weeks 1* and *4* ALDOST was reported by us previously (68).
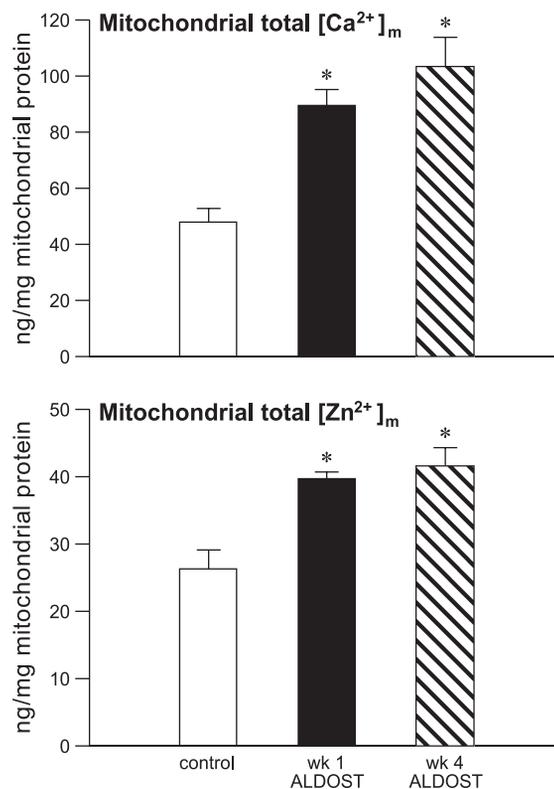

Fig. 2. Mitochondrial total $[Ca^{2+}]_m$ and $[Zn^{2+}]_m$ concentration harvested from control hearts as well as at 1- and 4-wk ALDOST. *$P < 0.05$ vs. controls.
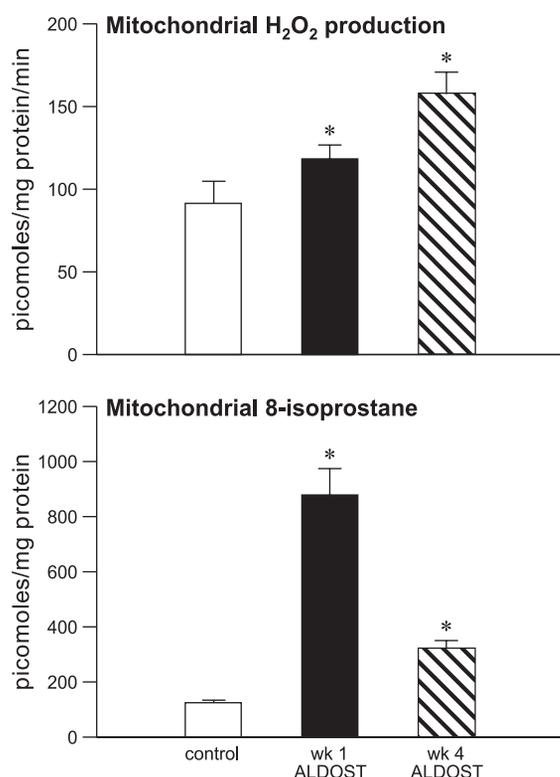
Mitochondrial H$_2$O$_2$ production

Mitochondrial 8-isoprostane

Fig. 3. Mitochondrial H$_2$O$_2$ production and 8-isoprostane levels in organelles harvested from control hearts as well as with 1- and 4-wk ALDOST. *$P < 0.05$ vs. controls.

GSHPx expression and activity. Analysis of microarray data showed a 10–20% increase in GSHPx mRNA at *weeks 1* and *4* ALDOST, respectively (Table 1). GSHPx activity (Fig. 5, *top*) was consistently elevated ($P < 0.05$) in cardiac myocytes at *week 1* (0.23 ± 0.02) and *week 4* (0.25 ± 0.01) ALDOST, respectively, vs. 0.19 ± 0.01 mU/mg protein in controls. Likewise, the GSHPx activity in cardiac mitochondria at *week 1* (5.95 ± 0.36) and *week 4* (5.10 ± 0.34) ALDOST, respectively, were also significantly elevated ($P < 0.05$) compared with controls (3.64 ± 0.25 mU/mg mitochondrial protein).

Cu/Zn-SOD and MnSOD activities. Cu/Zn SOD mRNA expression did not change with ALDOST (Table 1). However, Cu/Zn SOD activity in cardiomyocytes (Fig. 5, *bottom*) was increased ($P < 0.05$) during *weeks 1* and *4* ALDOST (28.7 ± 2.6 and 34.8 ± 3.9), respectively, compared with controls (22.9 ± 1.1 U/mg protein).

On the other hand, activity of mitochondrial MnSOD did not change significantly with ALDOST (data not shown).

Glutathione. Levels of GSSG in cardiac myocytes were elevated at *weeks 1* and *4* ALDOST (1.86 ± 0.34 and 2.04 ± 0.32 nmol/mg protein, respectively, vs. 1.57 ± 0.12 in controls), reflecting a persistent increase in oxidative stress. A compensatory increase in reduced and total glutathione also occurred at *week 1* (10.1 ± 0.7) and *week 4* (9.6 ± 1.02), respectively, compared with controls (6.04 ± 0.4 nmol/mg protein). However, the GSH-to-GSSG ratio did not change significantly (data not shown).

The mRNA levels for enzymes glutathione synthase and thioredoxin reductase were also elevated during ALDOST compared with controls (Table 1). Furthermore, a significant

upregulation of glutathione *S*-transferase enzymes (GSTs) was seen with ALDOST (Table 1). GSTs catalyze the conjugation of GSSG, via the sulfhydryl group, to electrophilic centers on a wide variety of substrates. This activity is useful in the detoxification of endogenous compounds such as peroxidized lipids.

TAC. TAC embodies nonenzymatic low-molecular weight antioxidants and vitamins (A, C, and E). In cardiac myocytes, TAC was increased at *week 1* ALDOST, however, no further increase was observed at *week 4* despite continuing presence of oxidative stress suggesting that antioxidant reserves were overwhelmed (3.96 ± 0.6 and 3.15 ± 0.46 at *weeks 1* and *4*, respectively, vs. 1.87 ± 0.26 Trolox U/mg protein in controls). In contrast, mitochondrial TAC initially fell following 1-wk ALDOST but later returned to the control levels (control, 14.2 ± 2.06 vs. 9.9 ± 2.2 and 16.01 ± 1.6 at *weeks 1* and *4* ALDOST, respectively). These data putatively implicate a disproportionate rise in mitochondrial 8-isoprostane levels found at *week 1* compared with *week 4*, thus providing experimental evidence of the imbalance between pro- and antioxidant defenses during ALDOST.

mPTP opening. Mitochondrial Ca^{2+} overloading commensurate with the high cardiomyocyte cytosolic [Ca^{2+}]$_i$ levels may initiate the opening of a nonspecific pore in the inner mitochondrial membrane, the mPTP. This Ca^{2+}-dependent formation and regulation of the mPTP opening is followed by an abrupt increase in the permeability of solutes (<1,500 Da mol mass) that are normally impermeable to the mitochondrial inner membrane, causing osmotic swelling and rupture of the outer membrane with concomitant loss of mitochondrial proteins. We detected (Fig. 6) a marked increase in the Ca^{2+}-induced opening of mPTP in cardiac mitochondria isolated from ALDOST rats (ΔA_{520} 107.4 ± 9.3 at *week 4* ALDOST vs. 68.6 ± 9.5 in controls; $P < 0.05$).

DISCUSSION

The administration of a catecholamine or I/R injury each lead to acute Ca^{2+} overloading in cardiac myocytes and mitochondria, with a concomitant loss of high-energy-rich phosphates that account for irreversible structural damage of these organelles and subsequent necrosis of energy-starved cardiomyocytes. Based on monoclonal antimyosin antibody labeling studies, cardiomyocyte necrosis is evident within hours of
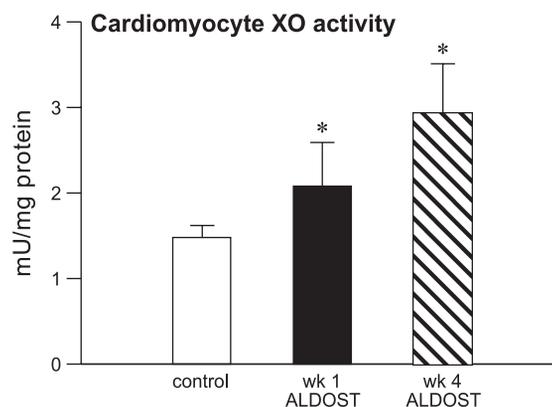
Cardiomyocyte XO activity

Fig. 4. Cardiomyocyte xanthine oxidase (XO) activity measured in cells harvested from control hearts as well as at *weeks 1* and *4* ALDOST. *$P < 0.05$ vs. controls.

Table 1. *mRNA expression of antioxidant enzymes*

	Control	ALDOST, 1 wk	ALDOST, 4 wk	Significance
Xanthine dehydrogenase	1.0 ± 0.0	1.6 ± 0.1	1.3 ± 0.1	$P < 0.05$
MT-1, mRNA	1.0 ± 0.2	1.5 ± 0.4	2.4 ± 0.2	$P < 0.05$
Glutathione synthase	1.0 ± 0.1	1.0 ± 0.1	1.5 ± 0.1	$P < 0.05$
Glutathione peroxidase	1.0 ± 0.0	1.1 ± 0.0	1.2 ± 0.0	$P < 0.05$
Glutathione *S*-transferase, α-type	1.0 ± 0.1	1.4 ± 0.2	1.4 ± 0.1	$P < 0.05$
Glutathione *S*-transferase, μ-type 2	1.0 ± 0.0	1.5 ± 0.0	1.6 ± 0.1	$P < 0.01$
Thioredoxin reductase 1	1.0 ± 0.1	1.5 ± 0.1	1.3 ± 0.1	$P < 0.05$
Cu/Zn-SOD	1.0 ± 0.0	1.0 ± 0.1	1.0 ± 0.0	NS
MnSOD	1.0 ± 0.0	0.9 ± 0.1	0.8 ± 0.1	NS

Aldosterone/salt treatment (ALDOST) 1- and 4-wk data are expressed as fold changes (means $\pm$ SE) relative to the normal controls, which were assigned a value of $1.00 \pm$ SE. *P* values compare control vs. 4-wk ALDOST. MT-1, metallothionein-1; NS, not significant.

isoproterenol administration (9, 32). Herein, we exploited our rat model of chronic ALDOST where intracellular Ca^{2+} overloading of cardiac myocytes and mitochondria was known to be present at *week 4* coincident with delayed myocardial necrosis and scarring (26, 66). The subacute intracellular Ca^{2+} overloading in this model is intrinsically coupled to increased intracellular Zn^{2+}, where Ca^{2+} and Zn^{2+} entry serve as prooxidant and antioxidant, respectively (44). The first objective of our study therefore was to determine the temporal responses in the coupled Ca^{2+} and Zn^{2+} dyshomeostasis that occur in these cells and organelles before the appearance of cardiac pathology (*week 1*) and during the ensuing pathological stage (*week 4*), together with their relevant biomarkers of oxidative stress and pathophysiological responses in antioxidant defenses.
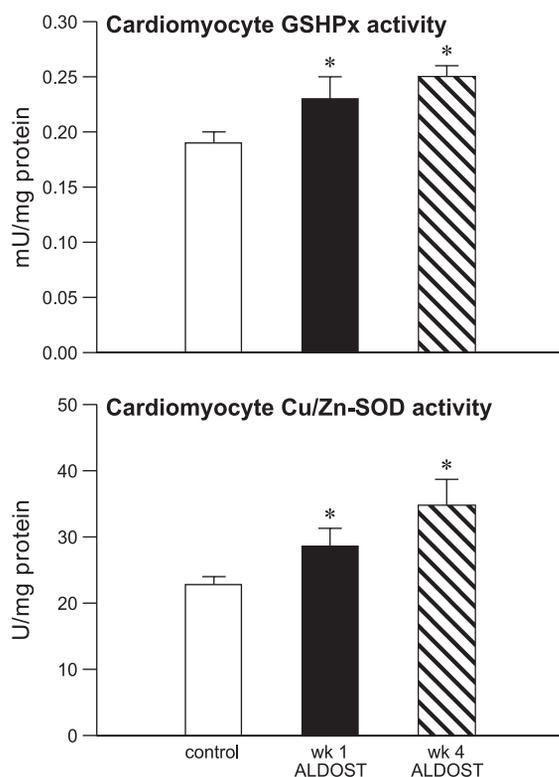

Fig. 5. Cardiomyocyte glutathione peroxidase (GSHPx) activity and Cu/Zn-SOD activity in cells harvested from control hearts as well as at *weeks 1* and *4* ALDOST. *$P < 0.05$.

We found that cytosolic free $[Ca^{2+}]_i$ and mitochondrial $[Ca^{2+}]_m$ in cardiomyocytes were already increased severalfold above the control values at *week 1* of ALDOST and remained significantly elevated at *week 4*. As we have previously reported, the rise in $[Ca^{2+}]_i$ occurs via L-type Ca^{2+} channels and is PTH-mediated; and ALDOST is indirectly responsible for these responses as it promotes SHPT via increased excretory Ca^{2+} losses with the contemporaneous appearance of ionized hypocalcemia (19, 44, 60, 69). The sustained elevation in $[Ca^{2+}]_m$ implicates the activation of a Na^+-dependent mitochondrial uniporter for which the primary function is to sequester Ca^{2+} under pathological stimuli (37). Michels and coworkers (53) have recently identified hitherto unknown Ca^{2+} selective channels in mitochondria obtained from nonfailing and failing human hearts, and their activity was significantly reduced in failing hearts due to impaired Ca^{2+} uptake. Relative to Ca^{2+} efflux, Smogorzewski et al. (62) found Ca^{2+}-ATPase-mediated extrusion of Ca^{2+} from cardiomyocytes to be reduced with SHPT, which further contributes to intracellular Ca^{2+} overloading. Mitochondrial Ca^{2+} extrusion is mediated by Na^+-Ca^{2+} exchanger located in the inner membrane (35). It is presently uncertain whether the function of this exchanger is altered during ALDOST, although the role of mitochondrial Na^+-Ca^{2+} exchanger in the pathophysiological expression of dystrophic cardiomyopathy has been previously studied by one
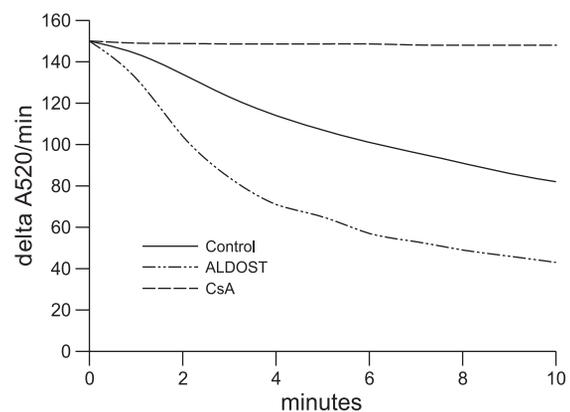

Fig. 6. Mitochondrial swelling was induced by 200 μmol/l $CaCl_2$. The decrease in changes in adsorption at 560 nm wavelength per minute (A560/min) rate of absorbance was plotted against time (minutes). Four-week ALDOST markedly increased mitochondrial transition pore opening compared with control. Mitochondrial transition pore opening was completely prevented by cyclosporine A (CsA).

of us (S. K. Bhattacharya). The early and persistent Ca^{2+} overloading of cardiac myocytes and their mitochondria was accompanied by a severalfold rise in $[Zn^{2+}]_i$ and $[Zn^{2+}]_m$ at *weeks 1* and *4* ALDOST, which we have shown to be associated with the increased expression of cardiomyocyte Zn^{2+} transporters induced by oxidative stress and preventable by cotreatment with spironolactone or amlodipine (44). Mechanisms of cardiac mitochondrial Zn^{2+} uptake remain to be fully elucidated. However, we speculate a transporter associated with the inner membrane would putatively involve a direct exchange between the Zn^{2+}-bound metallothionein chaperone complex with the transporter (22, 36).

At *week 1* ALDOST, the Ca^{2+} overloading of cardiac myocytes and mitochondria was accompanied by a significant rise in cardiomyocyte XO activity and mitochondrial H_2O_2 production together with an elevation in cardiac tissue 8-isoprostane level. However, this amplified prooxidant profile was also accompanied by simultaneous upregulated transcription of multiple antioxidant enzymes, including MT-1 and glutathione synthase, which was related to the activation of the Zn^{2+} sensor MTF-1 (5). Furthermore, the activity of antioxidant metalloenzymes was correspondingly increased, including Se-GSHPx and Cu/Zn-SOD, as was the level of GSSG and TAC, a marker of overall tissue nonenzymatic antioxidants including vitamins A, C, and E. We speculate our findings congruently point to an activation of inherent compensatory mechanisms that strive to achieve a balance between pro- and antioxidants at *week 1* ALDOST, thus abrogating or even preventing cardiomyocyte necrosis, since scarring was not evident by light microscopy until *week 4*.

Furthermore, at *week 4* ALDOST, and coincident with the delay in myocardial pathology [as reviewed elsewhere (66)], there was a marked rise in mitochondrial H_2O_2 production and tissue levels of 8-isoprostane, in keeping with the unbridled rate of lipid peroxidation, reflecting a dysequilibrium between the rate of superoxide formation and matrix H_2O_2 scavenging. This prooxidant state ensues in the absence of a proportional further increase in antioxidant defenses beyond that seen at *week 1* suggesting that antioxidant defenses were temporarily overwhelmed, including GSHPx activity and TAC. This evolving dysequilibrium between prooxidants and antioxidant defenses ultimately led to oxidative stress-induced cardiomyocyte necrosis and subsequent tissue repair with scarring first seen at *week 4*. We believe Ca^{2+} overloaded mitochondria are the likely initial source of oxidative stress in these cells, which then perpetuate to involve their cytosol, where other sources of ROS could be contributory. This sequence of events needs to be examined in future studies using a mitochondrial-specific antioxidant (74) or a specific mitochondrial Ca^{2+} uptake inhibitor (27).

In this context, mitochondria serve as an endogenous Ca^{2+} buffer mechanism regulating intracellular free Ca^{2+} concentrations within a narrow physiological threshold. The Na^+-dependent mitochondrial uniporter of the inner membrane is dominant in the heart and sequesters Ca^{2+} when cytosolic Ca^{2+} levels rise severalfold above the resting concentrations and such overloading is prolonged (37). In chronic ALDOST, the early and persistent Ca^{2+} overloading of cardiac mitochondria, a major site of ROS generation, plays a key role in the genesis of mitochondrial pathology (24, 43). The mPTP is a regulated Ca^{2+}-dependent opening of the inner membrane

transition pore that leads to a passive loss of membrane potential, ATP depletion, mitochondrial dysfunction with swelling and rupture of the outer membrane, and ultimately the necrosis of cardiomyocytes (41). Protecting mitochondria from oxidative stress-induced impairment offers an attractive and novel therapeutic approach. Unlike conventional antioxidants, which do not reach and penetrate these organelles, a mitochondria-specific antioxidant would provide a more targeted intervention (1, 34, 67, 74). An infiltration of inflammatory cells and myofibroblasts follows cardiomyocyte necrosis to restore the structural integrity of the myocardium with a replacement fibrosis or scarring. When ATP is available, the mPTP induces apoptosis, i.e., sterile cell death given an absence of inflammatory cells and fibroblast responses, where scarring is averted. We have not found evidence of apoptosis during ALDOST (unpublished observations), although others have and linked this to a concentration-dependent response to aldosterone (16). Cyclophilin D, an adenine nucleotide, regulates mPTP and necrotic cell death induced by intracellular Ca^{2+} overloading and H_2O_2 overproduction (6, 55). CsA binds directly to cyclophilin D to inhibit its activity and thereby prevents mPTP opening and parenchymal cell necrosis (15). Whether cotreatment with CsA or a nonimmunosuppressive analog of CsA would prevent cardiomyocyte necrosis during ALDOST remains to be investigated. Indirect measures that would reduce the accumulation of ROS within mitochondria and, in turn, block mPTP opening include divalent cations (Mg^{2+} and Mn^{2+}) (42). In this context, the mechanism underlying the reported cardioprotective role of a Zn^{2+} supplement
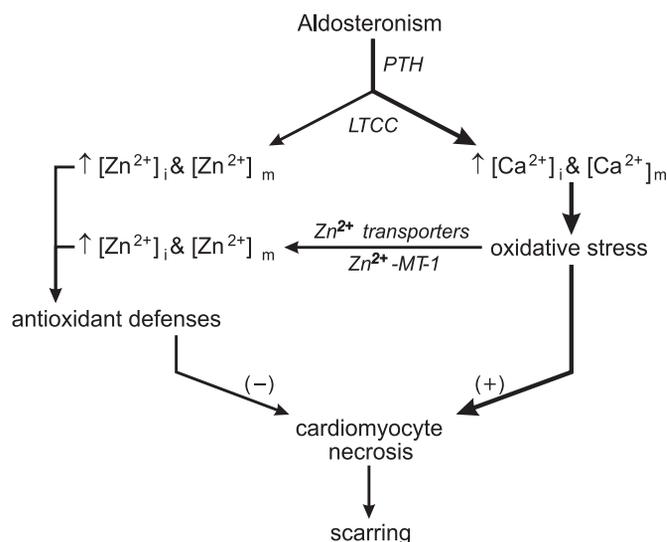
Fig. 7. Chronic aldosteronism involves the intrinsically coupled dyshomeostasis of Ca^{2+} and Zn^{2+} and includes cardiac myocytes and mitochondria that regulate the induction of oxidative stress and activation of endogenous antioxidant defenses. The accompanying intracellular Ca^{2+} overloading, which occurs via L-type Ca^{2+} channels (LTCC) and is mediated by parathyroid hormone (PTH), accounts for a rise in intracellular Zn^{2+} to a lesser extent. The excessive accumulation of intracellular Ca^{2+} and induction of oxidative stress activate the expression of membrane-bound Zn^{2+} transporters, the major route of Zn^{2+} entry, and the release of Zn^{2+} from the Zn^{2+}-metallothionein (MT)-1 complex. Collectively, increased intracellular Zn^{2+} contributes to antioxidant defenses. Persistent intracellular Ca^{2+} overloading, a result of chronic secondary hyperparathyroidism, accounts for the rate of oxidative stress exceeding (heavy line) antioxidant defenses. Cardiomyocyte necrosis with tissue repair and scarring are the end result.

in inhibiting mPTP opening needs to be further addressed, although the role of Zn^{2+} in maintaining intracellular redox homeostasis is well-established (49).

We acknowledge several limitations of our present study, which we plan to address in the future. We did not use electron microscopy to monitor ultrastructural aberrations in mitochondria at 4-wk ALDOST nor did we examine the respiratory functions, such as oxidative phosphorylation or ATP synthetic activity of cardiac mitochondria. To address the role of mitochondrial H_2O_2 generation and the effect of cyclophilin D on Ca^{2+}-activated mPTP-mediated cardiomyocyte necrosis, we plan to use a small peptide-based antioxidant that localizes to the mitochondrial inner membrane or CsA as cotreatment, respectively. Finally, we did not account for the potential transmural heterogeneity of Ca^{2+} channel population density across the myocardium or the heterogeneity of mitochondria found within the subsarcolemmal and interfibrillar spaces and their respective diversity in oxidative capacities (39, 48, 70).

Clinical correlates of our findings are severalfold. Elevation in serum PTH, the mediator of cardiomyocyte and mitochondrial EICA during aldosteronism (19, 26, 44), is present in patients hospitalized because of their symptoms and signs of CHF (4, 61). In outpatients with heart failure (reduced ejection fraction), serum PTH levels have recently been reported to be an independent predictor of the need for hospitalization for CHF (63). As demonstrated herein, EICA of aldosteronism is persistent and accompanied by a progressive rise in oxidative stress that overwhelms antioxidant defenses leading to the opening of the mPTP with ensuing necrotic cell death. Microscopic scarring, a footprint of previous necrosis, is present throughout the right and left ventricular myocardium of the explanted failing human heart (8, 23). Such diffuse scarring of the myocardium suggests ongoing cardiomyocyte necrosis; apoptosis does not beget a fibrous tissue response. In this context, an elevation in serum troponins, biomarkers of cardiomyocyte necrosis, has been reported in patients hospitalized with CHF in the absence of an acute coronary event or significant renal dysfunction and is associated with increased in-hospital and overall cardiac mortality (40, 47, 58, 73).

In summary and as depicted in Fig. 7, chronic ALDOST in rats is accompanied by intrinsically coupled dyshomeostasis of Ca^{2+} and Zn^{2+} in cardiac myocytes and mitochondria where they serve as pro- and antioxidants during its early preclinical (*week 1*) and pathological (*week 4*) stages, respectively. When endogenous antioxidant defenses are overwhelmed by oxidative stress, the resulting imbalance between pro- and antioxidants leads to cardiomyocyte necrosis and reparative fibrosis, eventuating in myocardial scarring. It is intriguing to postulate that this coupled dyshomeostasis could be pharmacologically uncoupled in favor of Zn^{2+} and antioxidant defenses, thus laying the foundation for novel cardioprotective strategies. Toward this end, a Zn^{2+} supplement or Zn^{2+} ionophore have each proven cardioprotective in the chronic stress models of ALDOST and streptozocin-induced diabetic cardiomyopathy, whereas the Zn^{2+} ionophore has been effective in the acute stressor states associated with I/R injury and isoproterenol administration (18, 20, 26, 46, 71).

DISCLOSURES

The authors have no conflicts of interest to disclose.

REFERENCES

1. **Adlam VJ, Harrison JC, Porteous CM, James AM, Smith RA, Murphy MP, Sammut IA.** Targeting an antioxidant to mitochondria decreases cardiac ischemia-reperfusion injury. *FASEB J* 19: 1088–1095, 2005.
2. **Ahokas RA, Sun Y, Bhattacharya SK, Gerling IC, Weber KT.** Aldosteronism and a proinflammatory vascular phenotype. Role of Mg^{2+}, Ca^{2+} and H_2O_2 in peripheral blood mononuclear cells. *Circulation* 111: 51–57, 2005.
3. **Ahokas RA, Warrington KJ, Gerling IC, Sun Y, Wodi LA, Herring PA, Lu L, Bhattacharya SK, Postlethwaite AE, Weber KT.** Aldosteronism and peripheral blood mononuclear cell activation. A neuroendocrine-immune interface. *Circ Res* 93: e124–e135, 2003.
4. **Alsafwah S, LaGuardia SP, Nelson MD, Battin DL, Newman KP, Carbone LD, Weber KT.** Hypovitaminosis D in African Americans residing in Memphis, Tennessee with and without heart failure. *Am J Med Sci* 335: 292–297, 2008.
5. **Andrews GK.** Regulation of metallothionein gene expression by oxidative stress and metal ions. *Biochem Pharmacol* 59: 95–104, 2000.
6. **Baines CP, Kaiser RA, Purcell NH, Blair NS, Osinska H, Hambleton MA, Brunskill EW, Sayen MR, Gottlieb RA, Dorn GW, Robbins J, Molkentin JD.** Loss of cyclophilin D reveals a critical role for mitochondrial permeability transition in cell death. *Nature* 434: 658–662, 2005.
7. **Baines CP, Song CX, Zheng YT, Wang GW, Zhang J, Wang OL, Guo Y, Bolli R, Cardwell EM, Ping P.** Protein kinase Cε interacts with and inhibits the permeability transition pore in cardiac mitochondria. *Circ Res* 92: 873–880, 2003.
8. **Beltrami CA, Finato N, Rocco M, Feruglio GA, Puricelli C, Cigola E, Quaini F, Sonnenblick EH, Olivetti G, Anversa P.** Structural basis of end-stage failure in ischemic cardiomyopathy in humans. *Circulation* 89: 151–163, 1994.
9. **Benjamin IJ, Jalil JE, Tan LB, Cho K, Weber KT, Clark WA.** Isoproterenol-induced myocardial fibrosis in relation to myocyte necrosis. *Circ Res* 65: 657–670, 1989.
10. **Bhattacharya SK, Crawford AJ, Thakar JH, Johnson PL.** Pathogenetic roles of intracellular calcium and magnesium in membrane-mediated progressive muscle degeneration in Duchenne muscular dystrophy. In: *Cell Calcium Metabolism: Physiology, Biochemistry, Pharmacology, and Clinical Implications*, edited by Fiskum G. New York: Plenum Press, 1989, p. 513–525.
11. **Bhattacharya SK, Johnson PL, Thakar JH.** Reversal of impaired oxidative phosphorylation and calcium overloading in the in vitro cardiac mitochondria of CHF-146 dystrophic hamsters with hereditary muscular dystrophy. *J Neurol Sci* 120: 180–186, 1993.
12. **Bhattacharya SK, Palmieri GM, Bertorini TE, Nutting DF.** The effects of diltiazem in dystrophic hamsters. *Muscle Nerve* 5: 73–78, 1982.
13. **Brilla CG, Pick R, Tan LB, Janicki JS, Weber KT.** Remodeling of the rat right and left ventricle in experimental hypertension. *Circ Res* 67: 1355–1364, 1990.
14. **Brilla CG, Weber KT.** Mineralocorticoid excess, dietary sodium and myocardial fibrosis. *J Lab Clin Med* 120: 893–901, 1992.
15. **Broekemeier KM, Dempsey ME, Pfeiffer DR.** Cyclosporin A is a potent inhibitor of the inner membrane permeability transition in liver mitochondria. *J Biol Chem* 264: 7826–7830, 1989.
16. **Burniston JG, Saini A, Tan LB, Goldspink DF.** Aldosterone induces myocyte apoptosis in the heart and skeletal muscles of rats in vivo. *J Mol Cell Cardiol* 39: 395–399, 2005.
17. **Cappuccio FP, Markandu ND, MacGregor GA.** Renal handling of calcium and phosphate during mineralocorticoid administration in normal subjects. *Nephron* 48: 280–283, 1988.
18. **Chanoit G, Lee S, Xi J, Zhu M, McIntosh RA, Mueller RA, Norfleet EA, Xu Z.** Exogenous zinc protects cardiac cells from reperfusion injury by targeting mitochondrial permeability transition pore through inactivation of glycogen synthase kinase-3β. *Am J Physiol Heart Circ Physiol* 295: H1227–H1233, 2008.

19. **Chhokar VS, Sun Y, Bhattacharya SK, Ahokas RA, Myers LK, Xing Z, Smith RA, Gerling IC, Weber KT.** Hyperparathyroidism and the calcium paradox of aldosteronism. *Circulation* 111: 871–878, 2005.
20. **Chvapil M, Owen JA.** Effect of zinc on acute and chronic isoproterenol induced heart injury. *J Mol Cell Cardiol* 9: 151–159, 1977.
21. **Corte ED, Stirpe F.** The regulation of rat liver xanthine oxidase. Involvement of thiol groups in the conversion of the enzyme activity from dehydrogenase (type D) into oxidase (type O) and purification of the enzyme. *Biochem J* 126: 739–745, 1972.
22. **Costello LC, Guan Z, Franklin RB, Feng P.** Metallothionein can function as a chaperone for zinc uptake transport into prostate and liver mitochondria. *J Inorg Biochem* 98: 664–666, 2004.
23. **Cotran RS, Kumar V, Robbins SL.** The heart. In: *Robbins Pathologic Basis of Disease* (4th ed.), edited by Cotran RS, Kumar V, and Robbins SL. Philadelphia: Saunders, 1989, p. 597–656.
24. **Duchen MR.** Mitochondria and Ca^{2+} in cell physiology and pathophysiology. *Cell Calcium* 28: 339–348, 2000.
25. **Fleckenstein A.** [Experimental pathology of the acute and chronic cardiac insufficiency.] *Verh Dtsch Ges Kreislaufforsch* 34: 15–34, 1968.
26. **Gandhi MS, Deshmukh PA, Kamalov G, Zhao T, Zhao W, Whaley JT, Tichy JR, Bhattacharya SK, Ahokas RA, Sun Y, Gerling IC, Weber KT.** Causes and consequences of zinc dyshomeostasis in rats with chronic aldosteronism. *J Cardiovasc Pharmacol* 52: 245–252, 2008.
27. **García-Rivas Gde J, Carvajal K, Correa F, Zazueta C.** Ru360, a specific mitochondrial calcium uptake inhibitor, improves cardiac postischaemic functional recovery in rats in vivo. *Br J Pharmacol* 149: 829–837, 2006.
28. **Garnier A, Bendall JK, Fuchs S, Escoubet B, Rochais F, Hoerter J, Nehme J, Ambroisine ML, De Angelis N, Morineau G, d'Estienne P, Fischmeister R, Heymes C, Pinet F, Delcayre C.** Cardiac specific increase in aldosterone production induces coronary dysfunction in aldosterone synthase-transgenic mice. *Circulation* 110: 1819–1825, 2004.
29. **Gehr MK, Goldberg M.** Hypercalciuria of mineralocorticoid escape: clearance and micropuncture studies in the rat. *Am J Physiol Renal Fluid Electrolyte Physiol* 251: F879–F888, 1986.
30. **Gerling IC, Singh S, Lenchik NI, Marshall DR, Wu J.** New data analysis and mining approaches identify unique proteome and transcriptome markers of susceptibility to autoimmune diabetes. *Mol Cell Proteomics* 5: 293–305, 2006.
31. **Gerling IC, Sun Y, Ahokas RA, Wodi LA, Bhattacharya SK, Warrington KJ, Postlethwaite AE, Weber KT.** Aldosteronism: an immunostimulatory state precedes the proinflammatory/fibrogenic cardiac phenotype. *Am J Physiol Heart Circ Physiol* 285: H813–H821, 2003.
32. **Goldspink DF, Burniston JG, Ellison GM, Clark WA, Tan LB.** Catecholamine-induced apoptosis and necrosis in cardiac and skeletal myocytes of the rat in vivo: the same or separate death pathways? *Exp Physiol* 89: 407–416, 2004.
33. **Goodwin KD, Ahokas RA, Bhattacharya SK, Sun Y, Gerling IC, Weber KT.** Preventing oxidative stress in rats with aldosteronism by calcitriol and dietary calcium and magnesium supplements. *Am J Med Sci* 332: 73–78, 2006.
34. **Graham D, Huynh NN, Hamilton CA, Beattie E, Smith RA, Cochemé HM, Murphy MP, Dominiczak AF.** Mitochondria-targeted antioxidant MitoQ10 improves endothelial function and attenuates cardiac hypertrophy. *Hypertension* 54: 322–328, 2009.
35. **Griffiths EJ.** Mitochondrial calcium transport in the heart: physiological and pathological roles. *J Mol Cell Cardiol* 46: 789–803, 2009.
36. **Guan Z, Kukoyi B, Feng P, Kennedy MC, Franklin RB, Costello LC.** Kinetic identification of a mitochondrial zinc uptake transport process in prostate cells. *J Inorg Biochem* 97: 199–206, 2003.
37. **Gunter TE, Buntinas L, Sparagna G, Eliseev R, Gunter K.** Mitochondrial calcium transport: mechanisms and functions. *Cell Calcium* 28: 285–296, 2000.
38. **Halestrap AP.** Calcium, mitochondria and reperfusion injury: a pore way to die. *Biochem Soc Trans* 34: 232–237, 2006.
39. **Hoppel CL, Tandler B, Parland W, Turkaly JS, Albers LD.** Hamster cardiomyopathy. A defect in oxidative phosphorylation in the cardiac interfibrillar mitochondria. *J Biol Chem* 257: 1540–1548, 1982.
40. **Ishii J, Nomura M, Nakamura Y, Naruse H, Mori Y, Ishikawa T, Ando T, Kurokawa H, Kondo T, Nagamura Y, Ezaki K, Hishida H.** Risk stratification using a combination of cardiac troponin T and brain natriuretic peptide in patients hospitalized for worsening chronic heart failure. *Am J Cardiol* 89: 691–695, 2002.
41. **Javadov S, Karmazyn M.** Mitochondrial permeability transition pore opening as an endpoint to initiate cell death and as a putative target for cardioprotection. *Cell Physiol Biochem* 20: 1–22, 2007.
42. **Javadov S, Karmazyn M, Escobales N.** Mitochondrial permeability transition pore opening as a promising therapeutic target in cardiac diseases. *J Pharmacol Exp Ther* 330: 670–678, 2009.
43. **Jung C, Martins AS, Niggli E, Shirokova N.** Dystrophic cardiomyopathy: amplification of cellular damage by Ca^{2+} signalling and reactive oxygen species-generating pathways. *Cardiovasc Res* 77: 766–773, 2008.
44. **Kamalov G, Deshmukh PA, Baburyan NY, Gandhi MS, Johnson PL, Ahokas RA, Bhattacharya SK, Sun Y, Gerling IC, Weber KT.** Coupled calcium and zinc dyshomeostasis and oxidative stress in cardiac myocytes and mitochondria of rats with chronic aldosteronism. *J Cardiovasc Pharmacol* 53: 414–423, 2009.
45. **Kamalov G, Holewinski JP, Bhattacharya SK, Ahokas RA, Sun Y, Gerling IC, Weber KT.** Nutrient dyshomeostasis in congestive heart failure. *Am J Med Sci* 338: 28–33, 2009.
46. **Karagulova G, Yue Y, Moreyra A, Boutjdir M, Korichneva I.** Protective role of intracellular zinc in myocardial ischemia/reperfusion is associated with preservation of protein kinase C isoforms. *J Pharmacol Exp Ther* 321: 517–525, 2007.
47. **Kuwabara Y, Sato Y, Miyamoto T, Taniguchi R, Matsuoka T, Isoda K, Yamane K, Nishi K, Fujiwara H, Takatsu Y.** Persistently increased serum concentrations of cardiac troponin in patients with acutely decompensated heart failure are predictive of adverse outcomes. *Circ J* 71: 1047–1051, 2007.
48. **Lesnefsky EJ, Tandler B, Ye J, Slabe TJ, Turkaly J, Hoppel CL.** Myocardial ischemia decreases oxidative phosphorylation through cytochrome oxidase in subsarcolemmal mitochondria. *Am J Physiol Heart Circ Physiol* 273: H1544–H1554, 1997.
49. **Maret W.** Molecular aspects of human cellular zinc homeostasis: redox control of zinc potentials and zinc signals. *Biometals* 22: 149–157, 2009.
50. **Massry SG, Coburn JW, Chapman LW, Kleeman CR.** The effect of long-term desoxycorticosterone acetate administration on the renal excretion of calcium and magnesium. *J Lab Clin Med* 71: 212–219, 1968.
51. **McCord JM, Roy RS.** The pathophysiology of superoxide: roles in inflammation and ischemia. *Can J Physiol Pharmacol* 60: 1346–1352, 1982.
52. **McKelvey TG, Hollwarth ME, Granger DN, Engerson TD, Landler U, Jones HP.** Mechanisms of conversion of xanthine dehydrogenase to xanthine oxidase in ischemic rat liver and kidney. *Am J Physiol Gastrointest Liver Physiol* 254: G753–G760, 1988.
53. **Michels G, Khan IF, Endres-Becker J, Rottlaender D, Herzig S, Ruhparwar A, Wahlers T, Hoppe UC.** Regulation of the human cardiac mitochondrial Ca^{2+} uptake by 2 different voltage-gated Ca^{2+} channels. *Circulation* 119: 2435–2443, 2009.
54. **Mohanty JG, Jaffe JS, Schulman ES, Raible DG.** A highly sensitive fluorescent micro-assay of H_2O_2 release from activated human leukocytes using a dihydroxyphenoxazine derivative. *J Immunol Methods* 202: 133–141, 1997.
55. **Nakagawa T, Shimizu S, Watanabe T, Yamaguchi O, Otsu K, Yamagata H, Inohara H, Kubo T, Tsujimoto Y.** Cyclophilin D-dependent mitochondrial permeability transition regulates some necrotic but not apoptotic cell death. *Nature* 434: 652–658, 2005.
56. **Nakayama H, Chen X, Baines CP, Klevitsky R, Zhang X, Zhang H, Jaleel N, Chua BH, Hewett TE, Robbins J, Houser SR, Molkentin JD.** Ca^{2+}- and mitochondrial-dependent cardiomyocyte necrosis as a primary mediator of heart failure. *J Clin Invest* 117: 2431–2444, 2007.
57. **Palmieri GM, Nutting DF, Bhattacharya SK, Bertorini TE, Williams JC.** Parathyroid ablation in dystrophic hamsters. Effects on Ca content and histology of heart, diaphragm, and rectus femoris. *J Clin Invest* 68: 646–654, 1981.
58. **Peacock WF 4th, De Marco T, Fonarow GC, Diercks D, Wynne J, Apple FS, Wu AH.** Cardiac troponin and outcome in acute heart failure. *N Engl J Med* 358: 2117–2126, 2008.
58a.**Peters J, Schlüter T, Riegel T, Peters BS, Beineke A, Maschke U, Hosten N, Mullins JJ, Rettig R.** Lack of cardiac fibrosis in a new model of high prorenin hyperaldosteronism. *Am J Physiol Heart Circ Physiol* 297: H1845–H1852, 2009.
59. **Rastegar A, Agus Z, Connor TB, Goldberg M.** Renal handling of calcium and phosphate during mineralocorticoid "escape" in man. *Kidney Int* 2: 279–286, 1972.

60. **Selektor Y, Ahokas RA, Bhattacharya SK, Sun Y, Gerling IC, Weber KT.** Cinacalcet and the prevention of secondary hyperparathyroidism in rats with aldosteronism. *Am J Med Sci* 335: 105–110, 2008.
61. **Shane E, Mancini D, Aaronson K, Silverberg SJ, Seibel MJ, Addesso V, McMahon DJ.** Bone mass, vitamin D deficiency, and hyperparathyroidism in congestive heart failure. *Am J Med* 103: 197–207, 1997.
62. **Smogorzewski M, Zayed M, Zhang YB, Roe J, Massry SG.** Parathyroid hormone increases cytosolic calcium concentration in adult rat cardiac myocytes. *Am J Physiol Heart Circ Physiol* 264: H1998–H2006, 1993.
63. **Sugimoto T, Tanigawa T, Onishi K, Fujimoto N, Matsuda A, Nakamori S, Matsuoka K, Nakamura T, Koji T, Ito M.** Serum intact parathyroid hormone levels predict hospitalisation for heart failure. *Heart* 95: 395–398, 2009.
64. **Suki WN, Schwettmann RS, Rector FC Jr, Seldin DW.** Effect of chronic mineralocorticoid administration on calcium excretion in the rat. *Am J Physiol* 215: 71–74, 1968.
65. **Sun Y, Ramires FJ, Weber KT.** Fibrosis of atria and great vessels in response to angiotensin II or aldosterone infusion. *Cardiovasc Res* 35: 138–147, 1997.
66. **Sun Y, Zhang J, Lu L, Chen SS, Quinn MT, Weber KT.** Aldosterone-induced inflammation in the rat heart. Role of oxidative stress. *Am J Pathol* 161: 1773–1781, 2002.
67. **Tauskela JS.** MitoQ–a mitochondria-targeted antioxidant. *IDrugs* 10: 399–412, 2007.
68. **Thomas M, Vidal A, Bhattacharya SK, Ahokas RA, Sun Y, Gerling IC, Weber KT.** Zinc dyshomeostasis in rats with aldosteronism. Response to spironolactone. *Am J Physiol Heart Circ Physiol* 293: H2361–H2366, 2007.
69. **Vidal A, Sun Y, Bhattacharya SK, Ahokas RA, Gerling IC, Weber KT.** Calcium paradox of aldosteronism and the role of the parathyroid glands. *Am J Physiol Heart Circ Physiol* 290: H286–H294, 2006.
70. **Wang HS, Cohen IS.** Calcium channel heterogeneity in canine left ventricular myocytes. *J Physiol* 547: 825–833, 2003.
71. **Wang J, Song Y, Elsherif L, Song Z, Zhou G, Prabhu SD, Saari JT, Cai L.** Cardiac metallothionein induction plays the major role in the prevention of diabetic cardiomyopathy by zinc supplementation. *Circulation* 113: 544–554, 2006.
72. **Weber KT.** From inflammation to fibrosis: a stiff stretch of highway. *Hypertension* 43: 716–719, 2004.
73. **Zairis MN, Tsiaousis GZ, Georgilas AT, Makrygiannis SS, Adamopoulou EN, Handanis SM, Batika PC, Prekates AA, Velissaris D, Kouris NT, Mytas DZ, Babalis DK, Karidis KS, Foussas SG.** Multimarker strategy for the prediction of 31 days cardiac death in patients with acutely decompensated chronic heart failure. *Int J Cardiol*. In press.
74. **Zhao K, Zhao GM, Wu D, Soong Y, Birk AV, Schiller PW, Szeto HH.** Cell-permeable peptide antioxidants targeted to inner mitochondrial membrane inhibit mitochondrial swelling, oxidative cell death, and reperfusion injury. *J Biol Chem* 279: 34682–34690, 2004.
75. **Zikos D, Langman C, Gafter U, Delahaye B, Lau K.** Chronic DOCA treatment increases Ca absorption: role of hypercalciuria and vitamin D. *Am J Physiol Endocrinol Metab* 251: E279–E284, 1986.